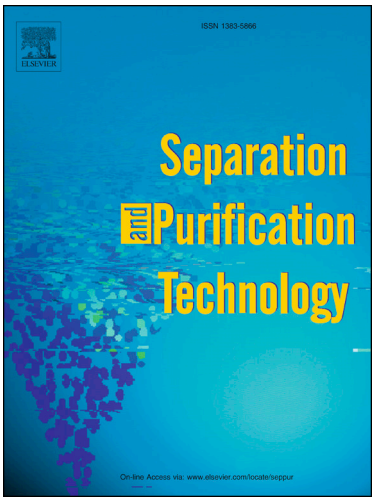

Membrane preconcentration as an efficient tool to reduce the energy consumption of perfluorohexanoic acid electrochemical treatment

Álvaro Soriano, Daniel Gorri, Ane Urtiaga

PII: S1383-5866(18)30374-5
DOI: https://doi.org/10.1016/j.seppur.2018.03.050
Reference: SEPPUR 14470

To appear in: *Separation and Purification Technology*

Received Date: 30 January 2018
Revised Date: 21 March 2018
Accepted Date: 23 March 2018

Please cite this article as: A. Soriano, D. Gorri, A. Urtiaga, Membrane preconcentration as an efficient tool to reduce the energy consumption of perfluorohexanoic acid electrochemical treatment, *Separation and Purification Technology* (2018), doi: https://doi.org/10.1016/j.seppur.2018.03.050

Membrane preconcentration as an efficient tool to reduce the energy consumption of perfluorohexanoic acid electrochemical treatment

Álvaro Soriano, Daniel Gorri, Ane Urtiaga*

Department of Chemical and Biomolecular Engineering, University of Cantabria

Av. de Los Castros s/n. 39005 Santander. Spain

*Corresponding author: urtiaga@unican.es

Revised manuscript

Submitted to *Separation and Purification Technology*

Special Issue: "Advanced Electrochemical Technologies for Environmental Applications"

March 2018

Abstract

One of the key points for the large-scale implementation of electrochemical water treatment technologies lies in the need of reducing the energy consumption. The present work analyzes the removal of persistent perfluorohexanoic acid (PFHxA, 204 $mg.L^{-1}$) from industrial process waters using a strategy that combines membrane pre-concentration followed by electrooxidation of the concentrate. A mathematical model describing the nanofiltration (NF) system was developed and complemented with new and background experimental data of PFHxA and ion species rejections and total permeate flux through the NF270 and NF90 membranes. Similarly, the kinetics of PFHxA electrolysis on boron doped diamond anodes was determined at laboratory scale. Later, the model was used to simulate the NF-ELOX integrated process, where a commercial spiral wound unit (membrane area 7.6 m^2) was implemented and the electrooxidation unit was scaled-up to pilot plant (anode area 1.05 m^2). The obtained energy savings depended on a combination of the target PFHxA removal ratio at the end of the treatment train, the separation performance of the commercial membrane and the reduction of the electrolyte ohmic resistance in the electrooxidation stage, that was attained as a result of the increase of salts content in the concentrate. Only the tight NF90 membrane allowed to achieve high (99%) PFHxA removal ratios in the integrated NF-ELOX process, and the specific energy consumption was estimated at 11.6 $kWh.m^{-3}$, 59.2% less than when electrolysis alone was applied. Still, the electrolysis is the most energy demanding step, with 85.9% contribution to the total energy consumption. The strategy of combining membrane pre-concentration with electrochemical degradation could be extended to the treatment of other highly persistent organic compounds.

Keywords: BDD electrolysis; energy minimization; nanofiltration; process integration; perfluorohexanoic acid

1. Introduction

Perfluoroalkyl substances (PFASs) are persistent organic pollutants that are recalcitrant to traditional water treatment technologies [1,2]. There is a growing concern about these substances due to their high bioaccumulation potential and their possible harmful effects on living beings [3,4]. Perfluorooctane sulfonate (PFOS) and its derivatives were classified as priority hazardous substances by the European water policy [5]. Recently, the European Regulation concerning Registration, Evaluation and Authorization of Chemicals (REACH), has fixed restrictions in the manufacturing for perfluorooctanoic acid (PFOA), its salts and PFOA-related substances [6]. The high concern about the persistence of PFASs have forced chemical manufacturers to substitute long-chain PFASs by their shorter-chain homologues [7]. Some alternatives, such as 6:2 fluorotelomer sulfonate (6:2 FTSA) and 6:2 fluorotelomer sulfonamide alkylbetaine (6:2 FTAB) are easily biodegradable, but their degradation products, among them perfluorohexanoic acid (PFHxA) being the most abundant, are still highly persistent [7,8].

Recently, electrochemical oxidation is gaining attention as an effective technology for the removal of PFASs [9–13]. However, so far the research is generally focused on degradation of PFOA and PFOS in model solutions, and the application of this technology to the treatment of PFASs in industrial effluents and real environmental matrixes is still at its beginning [11,13,14]. The main advantages of boron doped diamond (BDD) electrochemical oxidation (ELOX) for the abatement of persistent pollutants includes its high removal efficacy, mild temperature and pressure operation

conditions, ease of scale-up and automation [15–20]. Among the disadvantages, the high energy consumption stands as major drawback that hinder the large scale implementation of electrochemical technologies for water treatment. [16,19,21–24].

In search of innovations to achieve the energy optimization of environmental electrochemistry, this study is focused on the integration of pre-concentration strategies. The concentrations of PFASs in environmental media are usually very low [3,25], that leads to mass-transfer controlled electrooxidation kinetics, thus constraining the efficiency of the electrochemical process [21]. Pre-concentration strategies such as electrocoagulation [26] and membrane separation [14,27,28] have been proposed to overcome this limitation. Membrane separation such as nanofiltration (NF) and reverse osmosis could play a key role optimizing the electrochemical treatment of persistent PFASs due to the facts that: (i) it allows increasing PFASs concentration in the retentate whilst at the same time the volume to be electrolyzed is drastically reduced. In this way, higher feed concentrations promote the kinetics of diffusion controlled electrooxidation; (ii) not only PFASs, but also the concentration of salts naturally present in the water matrix will be increased, therefore decreasing the internal ohmic resistance of the electrolyte, which will make lower the cell voltage [29]; and (iii) higher concentration of dissolved ion species promotes the electrogeneration of oxidant species participating in indirect oxidation routes [30]. For example, the production of highly oxidative sulfate radical could contribute to the decomposition of PFCAs [31]. The first experimental attempt to integrate membrane separation and BDD electrolysis for PFHxA removal from industrial process waters showed that the energy consumption was reduced to 15.2 kWh m^{-3} for a 90% PFHxA removal ratio [14], a value that is significantly lower than energy requirements previously reported for PFASs electrochemical treatment, in the range 41.7 - 76.6 kWh m^{-3} [32]. The efficient PFHxA mineralization was confirmed by

the high reduction (>95%) of the total organic carbon (TOC). The selected nanofiltration membrane, the NF270 from Dow/Filmtec, was characterized by its very high productivity and its medium to high salt passage but the PFHxA retention might be insufficient when higher PFHxA removal ratios at the exit of the treatment train are required. Tighter NF or RO membranes could be useful to achieve this goal, usually at the expense of lower permeate fluxes. Also, our previous experimental work did not carry out any comprehensive assessment of the true impact of different membrane pre-concentration ratios on the energy consumption of the integrated process and on the contribution of each individual process on the overall energy demand. In this way, the modelling tools presented herein could help to quantitative select the appropriate operation variables thus providing knowledge that allows to move towards the definition of an optimized integrated process.

The aim of this study was to develop a methodology for the optimal integration of membrane separation and electrochemical oxidation for the treatment of waters impacted by persistent organic pollutants, with the objective of minimizing the energy consumption of the integrated NF-ELOX process. As a case of study, the removal and degradation of PFHxA will be analyzed. A global scheme of the proposed strategy is shown in Fig. 1. A mathematical model describing the membrane separation and the ELOX processes enabled the simulation of both technologies at pilot scale. Commercial spiral wound membrane modules and a battery of serial-parallel electrochemical cells were implemented in the simulations. The contribution of the two technologies to the total energy consumption was also analyzed.

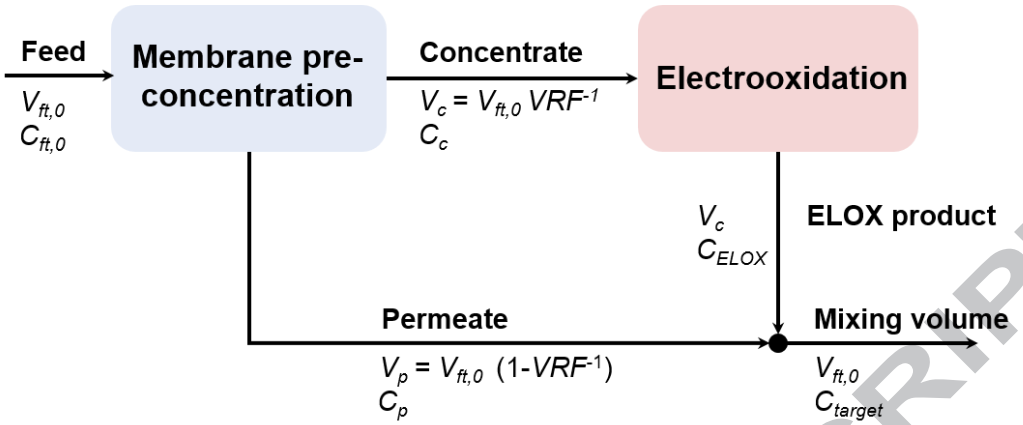

Fig. 1. **(1.5-column image)** Global scheme of the proposed NF-ELOX process

2. Methods

2.1 *Chemicals and materials*

All chemicals were analytical grade. Perfluorohexanoic acid (≥ 97%) was purchased from Sigma-Aldrich. Sodium chloride (≥ 99%), sodium hydroxide solution (1 N) and hydrochloric acid solution (1 N) were purchased from Panreac. Calcium sulphate dihydrate (≥ 98%) and methanol, UHPLC-MS (≥ 99.9%) were purchased from Scharlau. All solutions were prepared using ultrapure water (Milli-Q, Millipore).

Model solutions were prepared emulating real process waters previously studied [14], which were process streams in an industrial manufacturing process. The main process water characteristics are summarized in Table 1.

Table 1. Feed water characteristics

PFHxA	204 mg.L^{-1}
SO_4^{2-}	321 mg.L^{-1}
Cl^-	19.8 mg.L^{-1}
Ca^{2+}	172 mg.L^{-1}
Na^+	24.9 mg.L^{-1}

2.2 *Analytical methods*

An ultra-performance liquid chromatography (UPLC) system (Acquity H-Class, Waters) coupled with a triple quadrupole mass spectrometer (Acquity TDQ detector, Waters) and a column Acquity UPLC BEH C18 (1.7 µm, 2.1 × 50 mm) were used for the analysis of PFHxA at experiments carried out for the characterization of the NF90 membrane. A 2 mM ammonium acetate and 5% methanol aqueous solution and pure methanol were used as mobile phases at a flow rate of 0.15 $mL.min^{-1}$.

2.3 *Background data*

Previous NF experiments at laboratory-scale treating real industrial process streams [14] provided information about NF270 (Dow Filmtec) membrane permeability, rejections of PFHxA and ions in solution, as well as empirical correlations between PFHxA and ions concentrations in the retentate ($C_{r,i}$) and permeate ($C_{p,i}$) streams. The kinetic constant for the electrochemical degradation of PFHxA by means of BDD anodes at a working current density (J) of 50 A m^{-2} was also obtained ($k = 2.1 \times 10^{-3}$ $m.min^{-1}$).

In the present study, further experiments were conducted to characterize the tighter NF90 membrane (Dow Filmtec) using model solutions emulating the process waters described in Table 1. PFHxA concentration was varied in the range 100 - 500 $mg.L^{-1}$. Solutions were adjusted to neutral pH by adding sodium hydroxide 0.1 M and hydrochloric acid 0.1 M. Experiments were carried out in a laboratory membrane cross-flow test cell (SEPA-CF, GE Osmonics). Membrane coupons were cut with an effective membrane area of 155 cm^2. Feed solution was maintained at 20 °C and the operating pressure was varied from 2.5 bar to 20 bar.

2.4 *System definition*

A global scheme of the integrated process is sketched in Fig. 2. The technologies were simulated in batch mode. In the NF set-up, the retentate stream was recycled to the feed tank while the permeate stream was collected in the permeate tank, both open to the atmosphere. In this way, the concentration of PFHxA in the feed increased over time, whilst the feed volume decreased during the filtration run. Two commercial spiral-wound membrane modules (NF270-4040 and NF90-4040) were simulated and compared.

The composition of the resulting concentrate was considered as the feed properties in the ELOX simulation. For the ELOX simulations, the characteristics of an existing ELOX pilot plant previously used by our research group [18,33] were considered. The pilot plant is composed of a battery of serial-parallel electrochemical cells with a total BDD anode surface of 1.05 m^2, each one with similar characteristics to the cell used in the laboratory experiments. The current density was set at 50 A m^{-2} since it had been previously determined to optimally degrade PFHxA from NF concentrates [14]. Table 2 collects information about the main characteristics and operating conditions considered for the simulation of both processes.

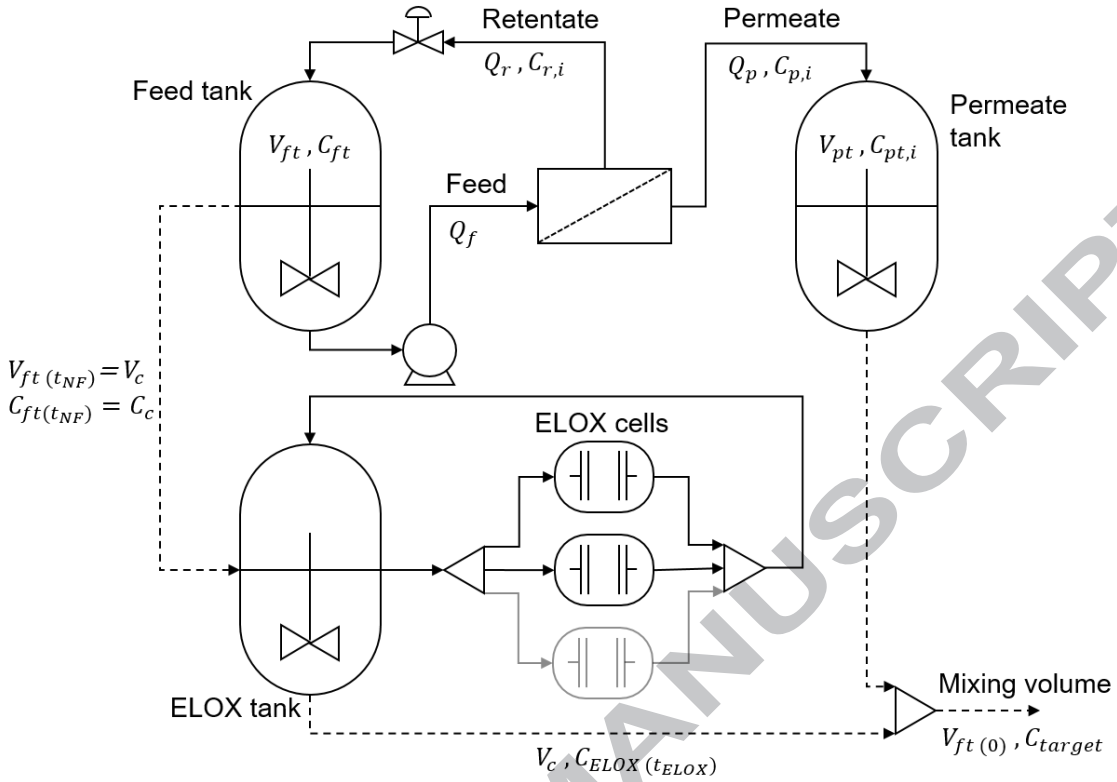

Fig. 2. (1.5 column image) Global scheme of the NF-ELOX integrated process. NF set-up with the commercial membrane module and ELOX of the NF concentrate using serial-parallel cells.

Table 2. Operating conditions and main characteristics of the system considered for the simulations.

Nanofiltration pilot plant	
Membrane area	7.6 m^2
Operating temperature	20ºC
Operating feed pressure	10 bar
Feed flow rate	3.6 m^3 h^{-1}
Initial feed tank volume	5 m^3
Electrooxidation pilot plant	
Total anode surface	1.05 m^2
Current density	50 A m^{-2}

2.5 *Process modelling*

All streams are assumed to be dilute solutions with constant density. The change in the volume of the feed and permeate tanks and the mass balances for the PFHxA solute, assuming perfect mixing, are written as follows,

$$\frac{dV_{ft}}{dt} = Q_r - Q_f \quad (1)$$

$$\frac{dV_{pt}}{dt} = Q_p \quad (2)$$

$$\frac{d(V_{ft}\, C_{ft,i})}{dt} = Q_r\, C_{r,i} - Q_f\, C_{ft,i} \quad (3)$$

$$\frac{d(V_{pt}\, C_{pt,i})}{dt} = Q_p\, C_{p,i} \quad (4)$$

Additionally, mass balances in the membrane module are defined as follows,

$$Q_f = Q_p + Q_r \quad (5)$$

$$Q_f\, C_{ft,i} = Q_p\, C_{p,i} + Q_r\, C_{r,i} \quad (6)$$

To solve the system of Eqs. (1-6) and predict the transport of solute and solvent across the membrane could require the use of rigorous transport models such as the Nernst-Planck equation [34] or empirical data. In this work we have used empirical data from concentration-mode laboratory experiments. The permeate volumetric flow rate (Q_p) can be related to the pressure gradient across the membrane and the membrane area, according to the following modified version of the Darcy's law,

$$Q_p = 10^{-3}\, L_p\, A\, (\Delta P - \Delta\pi) \quad (7)$$

In Eq. (7), L_p symbolizes the membrane permeability to the feed process waters under study and was empirically obtained for each membrane. The osmotic pressure difference between the feed and permeate streams have been calculated from the concentration of the dissolved species, using Eq. (8) [35].

$$\pi = 1.19\,(T + 273)\sum m_i \quad (8)$$

Furthermore, the volume reduction factor (*VRF*) is defined as the ratio between the initial feed volume and the concentrate final volume, which in this case corresponds to the volume of the feed tank at the end of the experimental run. This is an important operational variable and will be used in this work to study the influence of the membrane pre-concentration on the behavior of the integrated NF-ELOX process.

$$VRF = \frac{V_{ft}}{V_c} \quad (9)$$

The following PFHxA mass balance in the ELOX tank is valid under the assumption of negligible residence time of the fluid in the electrochemical cell compared to its residence time in the recirculation tank,

$$\frac{dC_{ELOX}}{dt} = -k\left(\frac{A_e}{V_c}\right)C_{ELOX} \quad (10)$$

From Fig. 2, it must be noticed that the final volume obtained after the treatment train, which is the same as the initial feed volume (V_{ft}), is the result of mixing the final permeate volume from the nanofiltration step (V_{pt}) and the treated electrooxidation volume, which is the same as the final concentrate volume from NF (V_c), for a certain *VRF*. Therefore, the PFHxA mass balance at the mixing point is written as in Eq. (11).

$$V_{ft}\,C_{target} = V_c\,C_{ELOX} + V_{pt}\,C_{pt,PFHxA} \quad (11)$$

As *VRF* is used as operational variable, Eq. (11) can be rearranged for the calculation of the required PFHxA concentration and required electrolysis time in the ELOX treatment

for meeting the target PFHxA concentration at the end of the treatment train under different *VRF*, after combining with Eq. (9),

$$C_{ELOX} = VRF\left[C_{target} - C_{pt,PFHxA}\,(1 - VRF^{-1})\right] \quad (12)$$

$$t_{ELOX} = \frac{ln(C_{ELOX}/C_c)\,V_{ft}}{-k\,A_e\,VRF\,60} \quad (13)$$

where 60 is a unit conversion factor (min h^{-1}). A simplified first approach to the NF energy consumption can be done by considering it equal to the work performed by the pump when it operates the time needed to reach a *VRF* value,

$$E_{NF} = \frac{Q_f\,\Delta P\,t_{NF}}{36\,\eta} \quad (14)$$

Where η is the global pumping system efficiency, including the pump and the electric motor efficiency, assumed to be 80% [36]. In Eq. (14), number 36 is a unit conversion factor and has units of bar W s Pa^{-1} kW^{-1} h^{-1}. On the other hand, the ELOX energy consumption was calculated as follows,

$$E_{ELOX} = 10^{-3}U\,I\,t_{ELOX} \quad (15)$$

where 10^{-3} has units of kW W^{-1}. The specific energy consumption of the integrated process (SEC_{total}) is the result of the NF energy consumption plus the ELOX energy consumption, per m^3 treated, to treat the total inlet feed volume, which is the same as the outlet product volume. In this way, we also calculated the specific energy consumption of both individual processes (SEC_{NF} and SEC_{ELOX}) related the total product. All model equations were numerically solved using Scilab. The equations were solved using the following initial conditions; $V_{ft}(0)$ = 5 m^3; $V_{pt}(0)$ = 0 m^3; $C_{ft,PFHxA}(0)$ =

204 mg.L^{-1}; $C_{ft,SO_4^{2-}}$ (0) = 321 mg.L^{-1}; $C_{ft,Ca^{2+}}$ (0) = 172 mg.L^{-1}; $C_{ft,\,Na^{+}}$ (0) = 24.9 mg.L^{-1}; $C_{ft,\,Cl^{-}}$ (0) = 19.8 mg.L^{-1}; $C_{i,pt}$ (0) = 0 mg.L^{-1}; C_{ELOX} (0) = C_c .

3. Results and discussion

3.1 *Experimental systems characterization*

In the present study, further experiments were conducted to characterize the tighter NF90 membrane (Dow Filmtec). Fig. 3a shows total permeate flux data as a function of the effective pressure gradient obtained for the NF90 membrane, using the feed process waters described in Table 1. The NF90 hydraulic permeability (L_p) was obtained from the slope of the linear regression. Fig. 3b provides the empirical correlation between the PFHxA concentrations in permeate and retentate streams at a fixed operating pressure of 10 bar, in experiments varying the feed concentration of PFHxA. In the same way, similar correlations were obtained for calcium, sulfate, chloride and sodium ions, all summarized in Table 3. For the NF90 membrane, these correlation equations correspond to the following average rejection factors [37]: R_{PFHxA} = 99.4%, R_{SO_4} = 98.8 ± 0.13%, $R_{Ca^{2+}}$ = 99.1 ± 0.18%, $R_{Na^{+}}$ = 98.5 ± 0.10%, $R_{Cl^{-}}$ = 93.6 ± 0.67%. In the same way, for the NF270 the average rejection factors of all species are: R_{PFHxA} = 95.7 ± 0.01%, R_{SO_4} = 96.1 ± 0.01%, $R_{Ca^{2+}}$ = 88.5 ± 0.01%, $R_{Na^{+}}$ = 67.9 ± 0.01%, $R_{Cl^{-}}$ = 41.7 ± 0.05%.

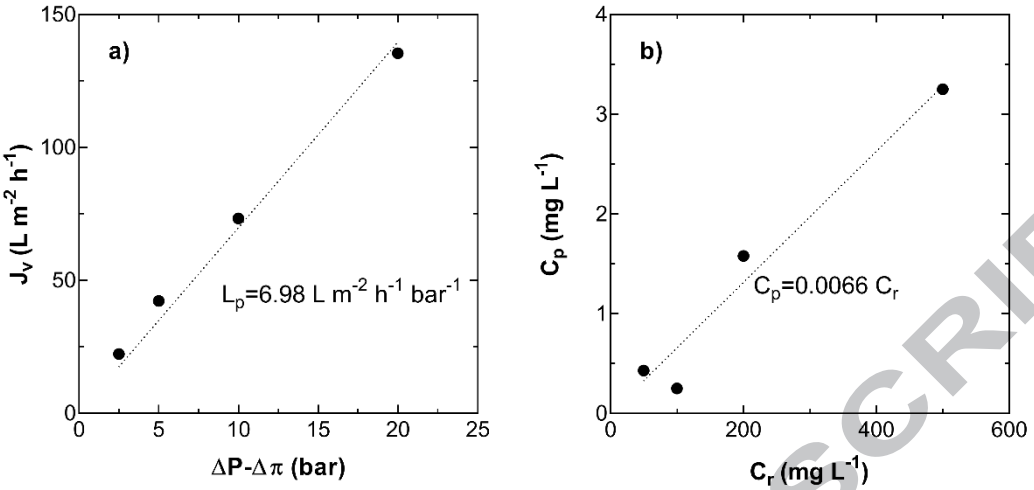

Fig. 3. **(1.5 column image)** a) Volumetric permeate flux through the NF90 membrane. Membrane permeability (L_p) is obtained from the slope. Feed composition as in Table 1; b) PFHxA concentration in the permeate vs. PFHxA in the retentate. ΔP = 10 bar.

Table 3. Empirical input data. NF270 and NF90 data determined at ΔP= 10 bar.

NF270 data	
Hydraulic permeability	L_p = 9.40 L m^{-2} h^{-1} bar^{-1}
$C_{p,,i}$-$C_{r,i}$ correlation	$C_{p,PFHxA} = 5.1\times10^{-2}\ C_{r,PFHxA}$
	$C_{p,SO_4^{2-}} = 3.7\times10^{-2}\ C_{r,SO_4^{2-}}$
	$C_{p,Ca^{2+}} = 11.4\times10^{-2}\ C_{r,Ca^{2+}}$
	$C_{p,Na^{+}} = 32.3\times10^{-2}\ C_{r,Na^{+}}$
	$C_{p,Cl^{-}} = 1.3\times10^{-2}\ (C_{r,Cl^{-}})^2 - 5.2\times10^{-2}\ C_{r,Cl^{-}}$
NF90 data	
Hydraulic permeability	L_p = 6.98 L m^{-2} h^{-1} bar^{-1}
$C_{p,,i}$-$C_{r,i}$ correlation	$C_{p,PFHxA} = 6.6\times10^{-3}\ C_{r,PFHxA}$
	$C_{p,SO_4^{2-}} = 4\times10^{-6}\ (C_{r,SO_4^{2-}})^2 + 8.3\times10^{-3}\ C_{r,SO_4^{2-}}$
	$C_{p,Ca^{2+}} = 5\times10^{-5}\ (C_{r,Ca^{2+}})^2 + 3.3\times10^{-3}\ C_{r,Ca^{2+}}$
	$C_{p,Na^{+}} = 2\times10^{-5}\ (C_{r,Na^{+}})^2 + 1.3\times10^{-2}\ C_{r,Na^{+}}$
	$C_{p,Cl^{-}} = 6.1\times10^{-2}\ C_{r,Cl^{-}}$
Electrooxidation data	
U - C_{eq} correlation	U (V) = 11.6 [C_{eq} (M) – 5.8 × 10^{-3}]$^{-4.8\times10^{-2}}$
PFHxA degradation kinetic constant	k = 2.1 × 10^{-3} m.min^{-1} (for J = 50 A.m^{-2})

Additionally, electrochemical experiments were carried out in galvanostatic conditions at J = 50 A.m^{-2} to characterize the effect of increasing the electrolyte concentration on

the cell voltage. The cell (DiaCell 201 PP, Adamant Technologies) was formed by two parallel flow-by compartments made of a central bipolar p-Si/ BDD electrode and p-Si/BDD anode and cathode. The total anodic area was 140 cm^2. 1 L saline feed solutions were prepared with calcium sulphate and sodium chloride with composition within the range of salts concentrations observed in the retentates of membrane experiments. The equivalent saline concentration ($C_{eq}= \frac{1}{2}\sum_{i=1}^{n}|z_i|C_i$) [34] was varied from 5.8×10^{-2} $mol.L^{-1}$ to 4.6×10^{-2} $mol.L^{-1}$. Fig. 4 shows how the cell voltage (U) can be moderately reduced as a result of the ohmic resistance decrease associated to the increase of the electrolyte concentration, although further reductions of the cell voltage are limited by the intrinsic resistances of the electrochemical cell. A good fit of the experimental data U vs. C_{eq} was obtained with a shifted power regression model, which was incorporated into the simulation runs (Table 3).

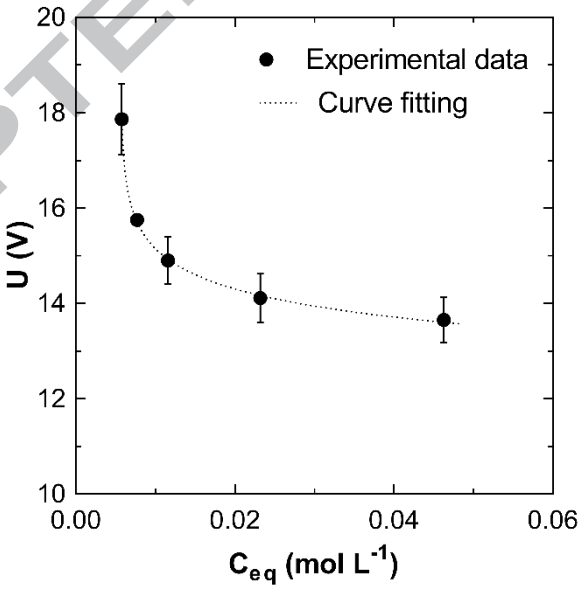

Fig. 4. **(single column image)** Cell voltage as function of the electrolyte concentration (C_{eq}). A bipolar BDD DiaCell 201 PP was used in the experiments.

3.2 *Membrane pre-concentration simulation*

Fig. 5 shows the simulation of the NF system. Simulations were run until *VRF* = 10, considering an initial feed volume of 5 m^3. As the feed volume V_{ft} keeps decreasing along the operation time, and as the NF270 and NF90 membranes are much more permeable to the solvent (water) than towards the solute (PFHxA), feed concentration C_{ft} and permeate tank concentration C_{pt} increases. The increase of salts concentration in the feed tank makes the osmotic pressure to increase too; as a result, the volumetric permeate flux Q_p decreases along the simulation run (Fig 5e). With the NF270 membrane and at *VRF* = 10, PFHxA concentration in the feed tank increased from 204 $mg.L^{-1}$ to 1779 $mg.L^{-1}$, after 6.7 h (Fig 5a). On the other hand, when the NF90 membrane unit is simulated, the PFHxA concentration in the feed tank increased to 2014 $mg.L^{-1}$ at *VRF* =10 after 9 h (Fig 5b). Thus, when the NF90 membrane is used, more time is needed to achieve the same *VRF*, as a result of its lower permeability. Overall, this property will increase the energy consumption of the pre-concentration step, but with the benefit of getting much lower PFHxA concentrations in the permeate tank than when using the NF270 membrane. Figs 5c and 5d show that at *VRF* = 10, the permeate tank PFHxA concentration with the NF90 membrane is 3.4 mg L^{-1}, while with the NF270 membrane its value is 30.7 $mg.L^{-1}$. The higher PFHxA concentration that is achieved in the permeate tank by using the NF270 membrane could be a detrimental factor in attaining the essential energy minimization objective. Also, the operation up to long filtration times and high *VRF* could clog the membrane pores due to the progressively higher solutes concentration, thus decreasing the permeate flux in a greater way in a real large-scale process, forcing to include periodical cleaning procedures. Increasing chloride concentration in the concentrate volume could also facilitate the potential formation of chlorate in the subsequent BDD anodic oxidation

treatment. Nevertheless, the process waters under study have a low chloride initial content (Table 1), being sulfate the major anion. On the other hand, nanofiltration membranes such as NF270 offer preferential retention of divalent anions (sulfate) over monovalent anions (chloride). As a result, Fig. 5 shows that chloride concentration in the retentate increased very little with the increase of *VRF*, also when working with the NF90 membrane. Additionally, the low current density selected for the electrooxidation of the concentrates (J=50 A m^{-2}) minimizes the potential chlorate formation in the electrolysis treatment [38].

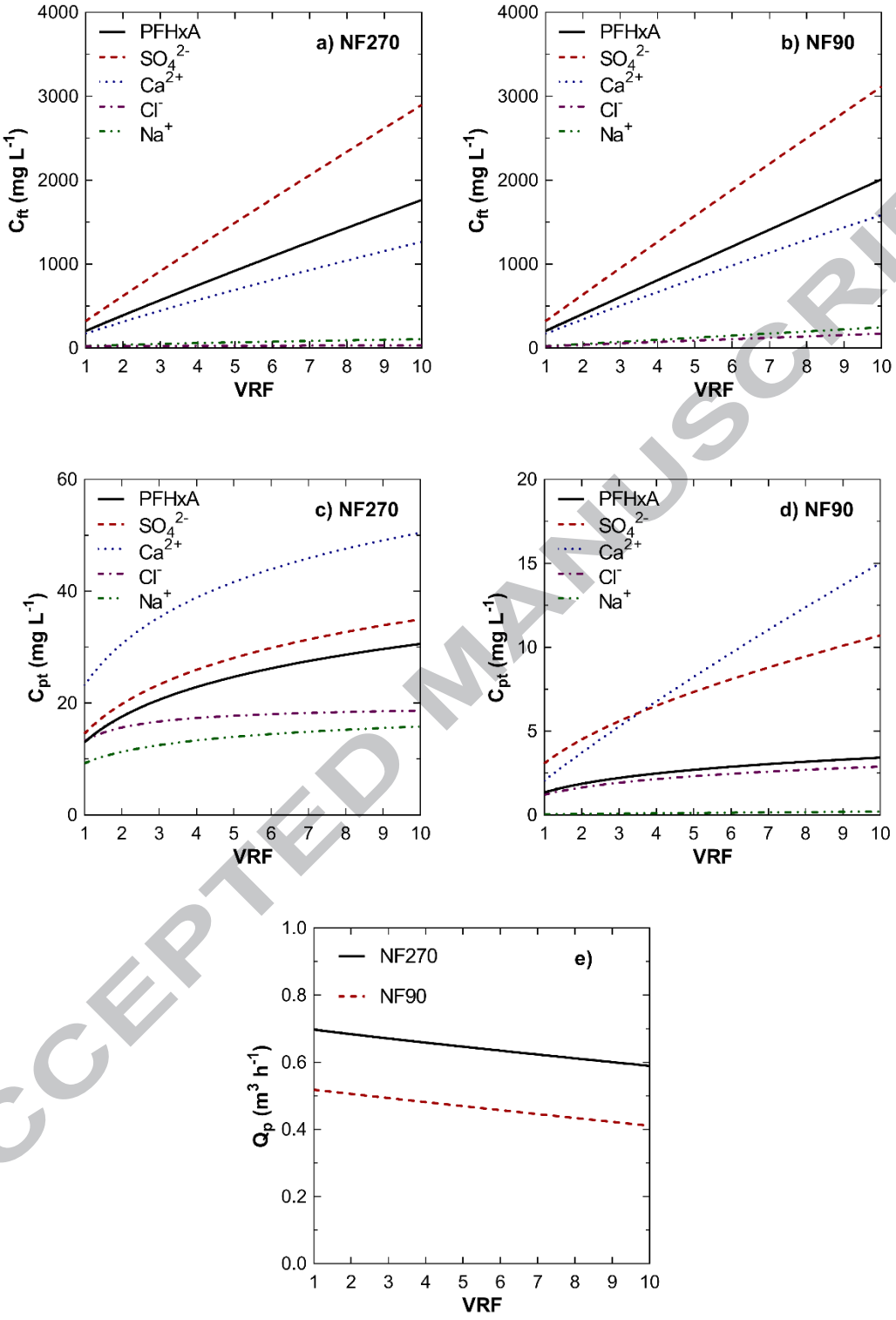

Fig. 5. (1.5 column image) Membrane pre-concentration simulations. PFHxA and ions concentration in the feed tank (a) and permeate tank (c) as a function of *VRF* with the NF270 membrane. PFHxA and ions concentration in the feed tank (b) and permeate tank (d) with the NF90 membrane. Permeate flux (e). Initial feed tank volume: 5 m^3.

3.3 *Effect of the NF pre-concentration on the electrooxidation stage and global process behavior*

Two different PFHxA target removal ratios (RR), RR = 90% and RR = 99%, were considered for the simulation runs of the electrooxidation stage and of the integrated NF-ELOX process. Fig. 6 shows the total energy consumption of the combined process per cubic meter of treated water as a function of the *VRF* parameter. *VRF* = 1 describes the situation in which no pre-concentration is carried out, i.e., ELOX is the only applied treatment. It is important to note that the maximum *VRF* value that is feasible to apply in the pre-concentration stage differs for the different scenarios under study. According to the PFHxA mass balance at the mixing point, Eq. (11), to meet a given C_{target} at the end of the treatment train, different C_{pt} and C_{ELOX} values are needed. With the increase of *VRF* (or analogously, with the increase of the nanofiltration pre-concentration operation time) the concentration in the permeate tank (C_{pt}) increases too, forcing the required C_{ELOX} at the exit of the electrooxidation stage to become lower, in order to meet C_{target} at the mixing point. Eventually C_{ELOX} will become equal to zero. At this point, *VRF* takes its maximum value.

For RR=90%, the use of ELOX alone consumes 14.3 kWh.m^{-3}, while the combination of NF270-ELOX minimizes the energy needs at a *VRF* = 4.0, with a specific energy consumption of 7.0 kWh.m^{-3}. Further energy savings can be obtained by using the NF90 membrane, that allows 90% PFHxA removal at a *VRF*=10 with only 3.3 kWh.m^{-3} When the target RR is set at 99%, the appropriate selection of the membrane module appears to be more important. The integration with the NF270 does not bring any benefit in terms of energy reduction. In fact, the pre-concentration step only contributes to increase the total energy demands of the system. In contrast, significant energy savings can be obtained with the NF90 –ELOX system. The energy consumption for the single

electrooxidation system (28.4 kWh.m^{-3}), is reduced to less than half (11.6 kWh.m^{-3}) by the integrated system.

Then, the different PFHxA rejections of the NF90 and NF270 membranes are a key performance parameter for the design and optimization of the integrated NF-ELOX process. When a low target concentration is demanded, the concentration in the membrane permeate stream needs to be low (Eq. 11), and the NF90 membrane fulfills this need at a much higher extent than the NF270 membrane. In the RR = 99% scenario and due to the insufficient NF270 PFHxA rejection, the PFHxA concentration in the permeate tank (C_{pt}) at initial time (12.9 mg.L^{-1}) is considerably higher than the objective C_{target} (2.0 mg.L^{-1}) and keeps increasing with the increase of *VRF*. The required C_{ELOX} at the exit of the electrooxidation stage to meet the PFHxA mass balance is therefore progressively smaller as *VRF* gets higher. Thus, the ELOX energy requirements to treat the NF concentrate to such low C_{ELOX} values are very high and keeps increasing with the simulation run. Conversely, the NF90 allows to obtain much lower PFHxA concentration in the permeate tank due to its higher PFHxA retention. For this reason, the required C_{ELOX} to meet the C_{target} is much less demanding and the ELOX energy consumption is reduced. The local minimum of the energy-*VRF* curve gives information on the optimal *VRF* value that allows maximum energy savings. When the target removal ratio is not so demanding (RR = 90%) the benefits of the NF-ELOX integration strategy can be clearly seen, and it is possible to apply longer NF pre-concentration times and thus higher *VRF* values with maximum energy savings in the process. For higher target removal ratios, only the NF90-ELOX combined strategy is able to reduce the energy consumption compared to the single electrooxidation process. Information about the optimal *VRF* for the different scenarios is gathered in Table 4. The reported energy consumption values of the ELOX treatment in all the studied scenarios are

significantly lower than the previously reported energy consumption of the electrochemical degradation of long-chain PFASs, in the range of 41.7 – 76.6 kWh m^{-3} [32], especially when the integration with the NF90 is carried out (1.3 -10.0 kW m^{-3} for RR = 90% and RR = 99%, respectively).

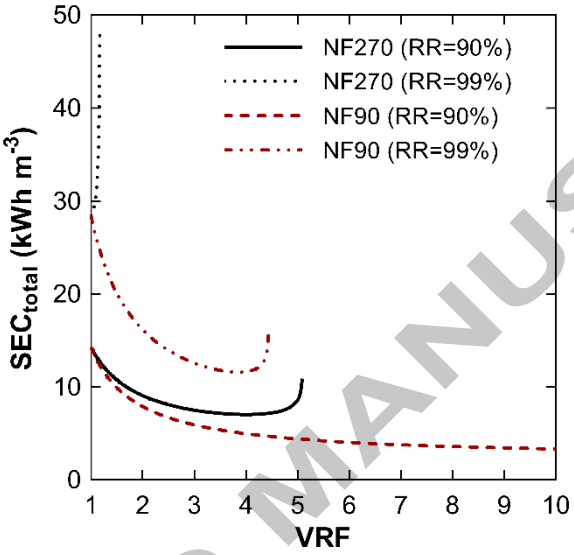

Fig. 6. (single column image) Specific energy consumption of the integrated NF-ELOX process as function of *VRF* for different PFHxA removal ratios at the end of the treatment train (RR = 90% and RR = 99%). V_{ft} = 5 m^3, $C_{f,0}$ = 204 mgL^{-1}.

Fig. 7 shows the contribution of the ELOX and membrane technologies to the total energy consumption, in two situations: i) first, when no pre-concentration is applied and only ELOX is considered for PFHxA removal; and ii) when the integrated process is considered and NF pre-concentration is applied using the optimal *VRF*, that is, the *VRF* that allows minimizing the energy consumption for each target removal ratio, as given in Fig. 6. For RR = 90%, the hybrid process consumes 50.6% (NF270) and 76.7% (NF90) less energy than the ELOX process alone. It is important to highlight that most of the energy consumption comes from the ELOX step. For RR = 99%, the integration

with the NF90 membrane is able to reduce the ELOX energy consumption by 64.9%. As the optimal *VRF* is limited to 3.9, the nanofiltration contribution to the total energy consumption is noticeably reduced. In this case, the hybrid process consumes 59.2% less energy than the ELOX process alone.

Table 4. Optimal variables allowing maximum energy savings in the integrated process.

Scenario	VRF	C_{ft}, NF (mg L^{-1})	C_{pt}, NF (mg L^{-1})	C_{ELOX} (mg L^{-1})	SEC_{NF} (kWh m^{-3})	SEC_{ELOX} (kWh m^{-3})
NF270 (RR=90%)	4.0	748.0	22.9	11.3	1.2	5.8
NF270 (RR=99%)	-	204.0	-	2.0	-	28.4
NF90 (RR=90%)	10.0	2014.1	3.4	169.6	2.0	1.3
NF90 (RR=99%)	3.9	778.7	2.4	0.7	1.6	10.0

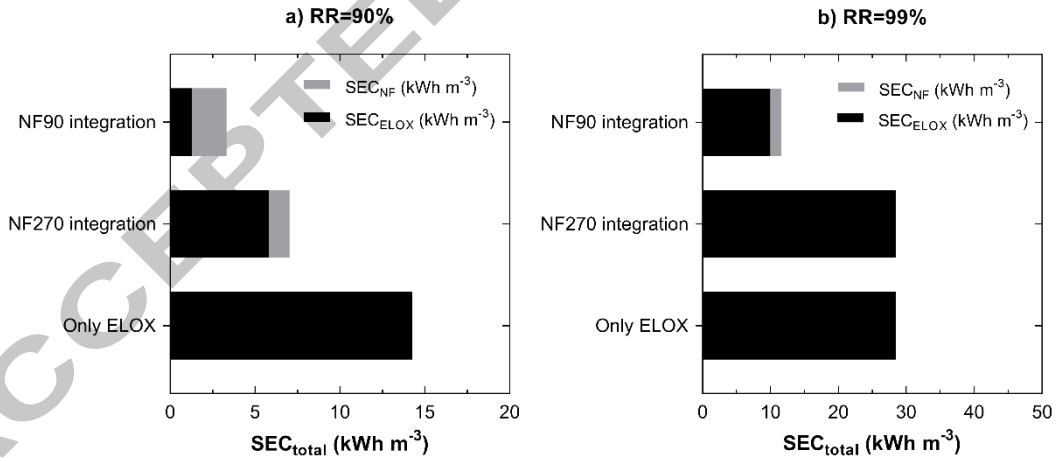

Fig. 7. (1.5 column image) Comparison of specific energy consumption when NF/ELOX are coupled at the optimal *VRF* and ELOX without previous NF pre-concentration are used, for the different PFHxA removal ratios. (a) RR=90%; (b) RR=99%.

4. Conclusions

The results presented herein stand out the integration of electrochemical technologies with membrane processes as a promising strategy to reduce the energy consumption of the electrochemical treatment of highly persistent organic pollutants in water. As a case of study, this work analyzed the removal of perfluorohexanoic acid from industrial process waters using a treatment train that combines nanofiltration and BDD electrochemical degradation of the concentrate stream obtained in the membrane separation unit. Mathematical simulation techniques, complemented by laboratory data of mass transfer parameters and electrolysis kinetics, were employed. In our case of study, the energy savings are clearly dependent on two factors: i) the final target PFHxA concentration in the treated water, that is, the ratio of PFHxA removal and ii) the permeability and rejection properties of the selected membrane. Thereof, the NF90 membrane followed by BDD electrooxidation allowed to achieve 76.7% and 59.2% energy savings for PFHxA removal ratios of 90% and 99%, compared to the direct BDD electrolysis. The use of a highly productive but less selective NF270 membrane provided 50.7% energy savings for a 90% removal ratio, although when the target removal ratio was raised to 99% the hybrid strategy did not bring any benefit. Also, it is relevant to point out that the contribution of NF to the process total energy consumption was the lowest in most cases. These results direct future research to the design of different membrane pre-concentration configurations. More sophisticated separations such as membrane cascade systems with multiple NF/RO stages and different recirculation and operation options could be useful to achieve higher purity in the permeate and lower electrooxidation requirements in an integrated process. However, the trade-off between PFHxA and ions selectivity and productivity should be taken into account. In this way, further optimization studies are needed as the way to exploit the

benefits of the integrated membrane separation-electrochemical treatment to reach high PFHxA removal ratios.

Acknowledgments

Financial support from projects CTM2013-44081-R, CTM2016-75509-R and CTQ2016-75158-R (MINECO, SPAIN-FEDER 2014–2020) and to the Spanish Excellence Network E3TECH (CTQ2015-71650-RDT) is gratefully acknowledged.

Nomenclature

A	Active membrane area (m^2)
A_e	Total anode area (m^2)
C_c	PFHxA concentration in the concentrate ($mg.L^{-1}$)
C_{ELOX}	Concentration in the ELOX reactor ($mg.L^{-1}$)
C_{eq}	Equivalent ion concentration ($mol\ L^{-1}$)
$C_{i,ft}$	Feed tank concentration ($mg.L^{-1}$)
$C_{i,p}$	Permeate stream concentration ($mg.L^{-1}$)
$C_{i,pt}$	Permeate tank concentration ($mg.L^{-1}$)
$C_{i,r}$	Retentate stream concentration ($mg.L^{-1}$)
C_{target}	PFHxA target concentration ($mg.L^{-1}$)
E_{ELOX}	ELOX energy consumption (kWh)
E_{NF}	NF energy consumption (kWh)
I	ELOX cell current intensity (A)
J	Current density ($A.m^{-2}$)
k	Kinetic constant ($m.min^{-1}$)
L_p	Membrane permeability ($L.m^{-2}.h^{-1}.bar^{-1}$)
m_i	Molality of the species dissolved ($mol.kg^{-1}$)
Q_f	Feed volumetric flow rate to NF module ($m^3.h^{-1}$)
Q_p	Permeate volumetric flow rate ($m^3.h^{-1}$)
Q_r	Retentate volumetric flow rate ($m^3.h^{-1}$)
SEC_{ELOX}	ELOX specific energy consumption ($kWh.m^{-3}$)
SEC_{NF}	NF specific energy consumption ($kWh.m^{-3}$)
SEC_{total}	Total specific energy consumption ($kWh.m^{-3}$)
T	Temperature of the solution (°C)
t_{ELOX}	ELOX operation time (h)
t_{NF}	NF operation time (h)
U	ELOX cell voltage (V)
V_c	Concentrate volume (m^3)
V_{ft}	Feed tank volume (m^3)
V_{pt}	Permeate tank volume (m^3)
VRF	Volume reduction factor (-)
z_i	Ionic valence (-)
ΔP	Effective pressure difference (bar)
$\Delta\pi$	Osmotic pressure difference (bar)
π	Osmotic pressure (bar)

References

[1] O.S. Arvaniti, A.S. Stasinakis, Review on the occurrence, fate and removal of perfluorinated compounds during wastewater treatment, Sci. Total Environ. 524–525 (2015) 81–92. doi:10.1016/j.scitotenv.2015.04.023.

[2] B. Gomez-Ruiz, P. Ribao, N. Diban, M.J. Rivero, I. Ortiz, A. Urtiaga, Photocatalytic degradation and mineralization of perfluorooctanoic acid (PFOA) using a composite TiO2−rGO catalyst, J. Hazard. Mater. 344 (2018) 950–957. doi:10.1016/j.jhazmat.2017.11.048.

[3] I. Fuertes, S. Gómez-Lavín, M.P. Elizalde, A. Urtiaga, Perfluorinated alkyl substances (PFASs) in northern Spain municipal solid waste landfill leachates, Chemosphere. 168 (2017) 399–407. doi:10.1016/j.chemosphere.2016.10.072.

[4] A.Y.C. Lin, S.C. Panchangam, Y.T. Tsai, T.H. Yu, Occurrence of perfluorinated compounds in the aquatic environment as found in science park effluent, river water, rainwater, sediments, and biotissues, Environ. Monit. Assess. 186 (2014) 3265–3275. doi:10.1007/s10661-014-3617-9.

[5] The European Parlament and the Council of the European Union, Directive 2013/39/EU of the Eruopean Parliament and of the council of 12 August 2013 amending Directives 2000/60/EC and 2008/105/EC as regards priority substances in the field of water policy, Off. J. Eur. Union. L 226/1 (2013) 1–17. doi:http://eur-lex.europa.eu/legal-content/EN/TXT/?uri=celex:32013L0039.

[6] The European Commission, Commission Regulation (EU) 2017/1000 of 13 June 2017: Amending Annex XVII to Regulation (EC) No 1907/ 2006 of the European Parliament and of the Council concerning the Registration, Evaluation,

Authorisation and Restriction of Chemicals (REACH) as regard, Off. J. Eur. Union. L 150 (2017) 14–18. http://eur-lex.europa.eu/legal-content/EN/TXT/PDF/?uri=CELEX:32017R1000&from=EN.

[7] Z. Wang, I.T. Cousins, M. Scheringer, K. Hungerbuehler, Hazard assessment of fluorinated alternatives to long-chain perfluoroalkyl acids (PFAAs) and their precursors: Status quo, ongoing challenges and possible solutions, Environ. Int. 75 (2015) 172–179. doi:10.1016/j.envint.2014.11.013.

[8] Z. Wang, I.T. Cousins, M. Scheringer, K. Hungerbühler, Fluorinated alternatives to long-chain perfluoroalkyl carboxylic acids (PFCAs), perfluoroalkane sulfonic acids (PFSAs) and their potential precursors, Environ. Int. 60 (2013) 242–248. doi:10.1016/j.envint.2013.08.021.

[9] B. Yang, C. Jiang, G. Yu, Q. Zhuo, S. Deng, J. Wu, H. Zhang, Highly efficient electrochemical degradation of perfluorooctanoic acid (PFOA) by F-doped Ti/SnO2 electrode, J. Hazard. Mater. 299 (2015) 417–424. doi:10.1016/j.jhazmat.2015.06.033.

[10] H. Lin, J. Niu, S. Ding, L. Zhang, Electrochemical degradation of perfluorooctanoic acid (PFOA) by Ti/SnO 2-Sb, Ti/SnO 2-Sb/PbO 2 and Ti/SnO 2-Sb/MnO 2 anodes, Water Res. 46 (2012) 2281–2289. doi:10.1016/j.watres.2012.01.053.

[11] C.E. Schaefer, C. Andaya, A. Burant, C.W. Condee, A. Urtiaga, T.J. Strathmann, C.P. Higgins, Electrochemical treatment of perfluorooctanoic acid and perfluorooctane sulfonate: insights into mechanisms and application to groundwater treatment, Chem. Eng. J. (2017). doi:10.1016/j.cej.2017.02.107.

[12] A. Urtiaga, C. Fernández-González, S. Gómez-Lavín, I. Ortiz, Kinetics of the electrochemical mineralization of perfluorooctanoic acid on ultrananocrystalline boron doped conductive diamond electrodes, Chemosphere. 129 (2015) 20–26. doi:10.1016/j.chemosphere.2014.05.090.

[13] C.E. Schaefer, C. Andaya, A. Urtiaga, E.R. McKenzie, C.P. Higgins, Electrochemical treatment of perfluorooctanoic acid (PFOA) and perfluorooctane sulfonic acid (PFOS) in groundwater impacted by aqueous film forming foams (AFFFs), J. Hazard. Mater. 295 (2015) 170–175. doi:10.1016/j.jhazmat.2015.04.024.

[14] Á. Soriano, D. Gorri, A. Urtiaga, Efficient treatment of perfluorohexanoic acid by nanofiltration followed by electrochemical degradation of the NF concentrate, Water Res. 112 (2017) 147–156. doi:10.1016/j.watres.2017.01.043.

[15] M. Panizza, G. Cerisola, Direct and mediated anodic oxidation of organic pollutants, Chem. Rev. 109 (2009) 6541–6569. doi:10.1021/cr9001319.

[16] C.A. Martínez-Huitle, M.A. Rodrigo, I. Sirés, O. Scialdone, Single and Coupled Electrochemical Processes and Reactors for the Abatement of Organic Water Pollutants: A Critical Review, Chem. Rev. 115 (2015) 13362–13407. doi:10.1021/acs.chemrev.5b00361.

[17] J. Muff, Chapter 3 – Electrochemical Oxidation – A Versatile Technique for Aqueous Organic Contaminant Degradation, in: Chem. Adv. Environ. Purif. Process. Water, 2014: pp. 75–134. doi:10.1016/B978-0-444-53178-0.00003-1.

[18] Á. Anglada, A.M. Urtiaga, I. Ortiz, Laboratory and pilot plant scale study on the electrochemical oxidation of landfill leachate, J. Hazard. Mater. 181 (2010) 729–

735. doi:10.1016/j.jhazmat.2010.05.073.

[19] A. Urtiaga, P. Gómez, A. Arruti, I. Ortiz, Electrochemical removal of tetrahydrofuran from industrial wastewaters: Anode selection and process scale-up, J. Chem. Technol. Biotechnol. 89 (2014) 1243–1250. doi:10.1002/jctb.4384.

[20] A. Urtiaga, P. Fernandez-Castro, P. Gómez, I. Ortiz, Remediation of wastewaters containing tetrahydrofuran. Study of the electrochemical mineralization on BDD electrodes, Chem. Eng. J. 239 (2014). doi:10.1016/j.cej.2013.11.028.

[21] J. Radjenovic, D.L. Sedlak, Challenges and Opportunities for Electrochemical Processes as Next-Generation Technologies for the Treatment of Contaminated Water, Environ. Sci. Technol. 49 (2015) 11292–11302. doi:10.1021/acs.est.5b02414.

[22] A. Anglada, D. Ortiz, A.M. Urtiaga, I. Ortiz, Electrochemical oxidation of landfill leachates at pilot scale: Evaluation of energy needs, Water Sci. Technol. 61 (2010) 2211–2217. doi:10.2166/wst.2010.130.

[23] A. Anglada, A. Urtiaga, I. Ortiz, Pilot Scale Performance of the Electro-Oxidation of Landfill Leachate at Boron-Doped Diamond Anodes, Environ. Sci. Technol. 43 (2009) 2035–2040. doi:10.1021/es802748c.

[24] Á. Anglada, A.M. Urtiaga, I. Ortiz, Laboratory and pilot plant scale study on the electrochemical oxidation of landfill leachate, J. Hazard. Mater. 181 (2010) 729–735. doi:10.1016/j.jhazmat.2010.05.073.

[25] T.G. Schwanz, M. Llorca, M. Farré, D. Barceló, Perfluoroalkyl substances assessment in drinking waters from Brazil, France and Spain, Sci. Total Environ.

539 (2016) 143–152. doi:10.1016/j.scitotenv.2015.08.034.

[26] J. Llanos, A. Raschitor, P. Cañizares, M.A. Rodrigo, Electrocoagulation as the Key for an Efficient Concentration and Removal of Oxyfluorfen from Liquid Wastes, Ind. Eng. Chem. Res. 56 (2017) 3091–3097. doi:10.1021/acs.iecr.7b00347.

[27] A.M. Urtiaga, G. Pérez, R. Ibáñez, I. Ortiz, Removal of pharmaceuticals from a WWTP secondary effluent by ultrafiltration/reverse osmosis followed by electrochemical oxidation of the RO concentrate, Desalination. 331 (2013) 26–34. doi:10.1016/j.desal.2013.10.010.

[28] H.T. Madsen, E.G. Søgaard, J. Muff, Reduction in energy consumption of electrochemical pesticide degradation through combination with membrane filtration, Chem. Eng. J. 276 (2015) 358–364. doi:10.1016/j.cej.2015.04.098.

[29] Á. Anglada, A. Urtiaga, I. Ortiz, Contributions of electrochemical oxidation to waste-water treatment: Fundamentals and review of applications, J. Chem. Technol. Biotechnol. 84 (2009) 1747–1755. doi:10.1002/jctb.2214.

[30] G. Pérez, A.R. Fernández-Alba, A.M. Urtiaga, I. Ortiz, Electro-oxidation of reverse osmosis concentrates generated in tertiary water treatment, Water Res. 44 (2010) 2763–2772. doi:http://dx.doi.org/10.1016/j.watres.2010.02.017.

[31] H. Hori, A. Yamamoto, E. Hayakawa, S. Taniyasu, N. Yamashita, S. Kutsuna, H. Kiatagawa, R. Arakawa, Efficient decomposition of environmentally persistent perfluorocarboxylic acids by use of persulfate as a photochemical oxidant, Environ. Sci. Technol. 39 (2005). doi:10.1021/es0484754.

[32] J. Niu, Y. Li, E. Shang, Z. Xu, J. Liu, Electrochemical oxidation of perfluorinated compounds in water, Chemosphere. 146 (2016) 526–538. doi:10.1016/j.chemosphere.2015.11.115.

[33] A. Anglada, R. Ibañez, A. Urtiaga, I. Ortiz, Electrochemical oxidation of saline industrial wastewaters using boron-doped diamond anodes, Catal. Today. 151 (2010) 178–184. doi:10.1016/j.cattod.2010.01.033.

[34] A. Pérez-González, R. Ibáñez, P. Gómez, A.M. Urtiaga, I. Ortiz, J.A. Irabien, Nanofiltration separation of polyvalent and monovalent anions in desalination brines, J. Memb. Sci. 473 (2015) 16–27. doi:http://dx.doi.org/10.1016/j.memsci.2014.08.045.

[35] T. Asano, Wastewater Reclamation and Reuse: Water Quality Management Library, CRC Press, Florida, 1998.

[36] F. Vince, F. Marechal, E. Aoustin, P. Bréant, Multi-objective optimization of RO desalination plants, Desalination. 222 (2008) 96–118. doi:10.1016/j.desal.2007.02.064.

[37] IUPAC, Terminology for membranes and membrane processes (IUPAC Recommendation 1996), J. Memb. Sci. 120 (1996) 149–159. doi:10.1016/0376-7388(96)82861-4.

[38] A.R.F. Pipi, I. Sirés, A.R. De Andrade, E. Brillas, Application of electrochemical advanced oxidation processes to the mineralization of the herbicide diuron, Chemosphere. 109 (2014) 49–55. doi:10.1016/j.chemosphere.2014.03.006.

Highlights

- Membrane pre-concentration was used to reduce electrooxidation energy needs
- Energy savings depend on the target removal rate and membrane type
- PFHxA was effectively removed by the integrated NF-electrolysis process
- NF90 membrane provided 60 - 71% energy savings for 99% and 90% removal ratios
- NF270 granted energy benefits only at 90% removal ratio

Graphical abstract